articles

molecular pharmaceutics

The Benefit of Hydrophobic Domain Asymmetry on the Efficacy of Transfection as Measured by *in Vivo* Imaging

Michael H. Nantz,[†] Christopher W. Dicus,[‡] Brendan Hilliard,[§] Sri Yellayi,[§] Shaomin Zou,[||] and James G. Hecker*[,||]

Department of Anesthesia and Critical Care, University of Pennsylvania, Philadelphia, Pennsylvania 19104-6112, Ampac Fine Chemicals, Sacramento, California, Department of Chemistry, University of Louisville, Louisville, Kentucky 40292, and Department of Pathology, University of Pennsylvania, Philadelphia, Pennsylvania 19104

Received November 30, 2009; Revised Manuscript Received March 5, 2010; Accepted March 16, 2010

Abstract: We, and others, have observed that the structure of cationic lipids appears to have a significant effect on the transfection efficacy of optimized nucleic acid/cationic lipid complexes (lipoplexes) used for *in vitro* and *in vivo* gene delivery and expression. Although there are many *in vitro* comparisons of lipid reagents for gene delivery, few comparisons have been made *in vivo*. We previously reported the effects of changes in hydrophobic domain chain length and chain asymmetry, changes in headgroup composition, and counterion exchange. We have observed in our own work over many years the apparent superiority of asymmetric versus symmetric hydrocarbon domains for otherwise similar lipids. In this investigation we use *in vivo* whole animal brain imaging to evaluate the contribution of symmetric versus asymmetric hydrophobic domains on what we previously determined to be optimal chain lengths for *in vitro* transfections. We specifically investigated several glycerol-based lipids; however, the rare reports of asymmetric non-glycerol-based lipids also support our observations. We found that asymmetric, two-chain cationic lipids of 14 to 18 carbons perform significantly better *in vivo*, as analyzed by whole animal imaging, than the paired symmetric lipids.

Keywords: Lipid-mediated; gene delivery; nonviral; gene therapy; lipid structure; asymmetry

Introduction

The efficiency of nonviral transfection of nucleic acids, particularly when using liposome formulations composed of cationic lipids, is dependent on numerous variables.[1−4] Since Felgner's seminal publications on the use of the prototype cationic lipid DOTMA as a vector for gene delivery to mammalian cells,[5,6] much effort has been devoted to understanding the relationship between lipid structure and transfection efficiency. Excellent reviews on structure−activity relationships in cationic lipid-mediated gene transfer are

* To whom correspondence should be addressed. Mailing address: University of Pennsylvania, Anesthesia and Critical Care, 305 Morgan Building, 3620 Hamilton Walk, Philadelphia, PA 19104-6112. Tel: (215) 349-5343. Fax: (215) 349-5078. E-mail: heckerj@uphs.upenn.edu.

[†] University of Louisville.

[‡] Ampac Fine Chemicals.

[§] Department of Pathology, University of Pennsylvania.

[||] Department of Anesthesia and Critical Care, University of Pennsylvania.

(1) Flotte, T. R. Gene Therapy: The First Two Decades and the Current State-of-the-Art. *J. Cell Physiol.* **2007**, *213*, 301–305.

(2) Karmali, P. P.; Chaudhuri, A. Cationic liposomes as non-viral carriers of gene medicines: Resolved issues, open questions, and future promises. *Med. Res. Rev.* **2007**, *27*, 696–722.

(3) Taira, K.; Kataoka, K.; Niidome, T. *Non-Viral Gene Therapy*; Springer-Verlag: Tokyo, 2005.

(4) Miller, A. D. Cationic Liposomes for Gene Therapy. *Angew. Chem., Int. Ed.* **1998**, *37*, 1769–1785.

(5) Felgner, P. L.; Gadek, T. R.; Holm, M.; Roman, R.; Chan, H. W.; Wenz, M.; Northrop, J. P.; Ringold, G. M.; Danielsen, M. Lipofection: A highly efficient, lipid-mediated DNA-transfection procedure. *Proc. Natl. Acad. Sci. U.S.A.* **1987**, *84* (21), 7413–7417.

(6) Felgner, J. H.; Kumar, R.; Sridhar, C. N.; Wheeler, C. J.; Tsai, Y.-J.; Border, R.; Ramsey, P.; Martin, M.; Felgner, P. L. Enhanced gene delivery and mechanism studies with a novel series of cationic lipid formulations. *J. Biol. Chem.* **1994**, *269*, 2550–2561.

10.1021/mp900298f
Published on Web 03/16/2010

available in refs 7 and 8. Regarding the commonly used glycerol-type dual chain lipids, such as DOTMA,[5] the most studied structural variables include compositions of the polar (DNA-binding)[6,9−13] and hydrophobic domains,[14,15] the chemical linkage used to connect the polar and hydrophobic domains (e.g., ether vs ester),[16−20] the nature of the anionic counterion,[21,22] and the nucleic acid to cationic lipid charge ratio.[23] Many structural permutations of these lipid variables have been created and, to some degree, studied. Of the transfection lipids now commercially available, all claim to have advantages in at least some *in vitro* cell types. However there are few independent comparisons of *in vitro* transfection and cytotoxicity results of commercially available lipids,[24] and even fewer that we are aware of *in vivo*.

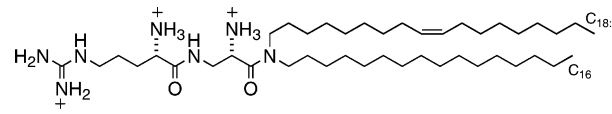

Figure 1. AtuFECT01.

Of the few reports on the use of dual-chain asymmetric transfection lipids for polynucleotide delivery *in vivo*, the non-glycerol-based lipids AtuFECT01 (Figure 1)[25] and lipid **4** (Table 3)[26] were examined for polynucleotide delivery to mouse vascular endothelium and mouse lung, respectively. To our knowledge there are no reports of asymmetric glycerol-based lipids for *in vivo* gene delivery other than our studies using MLRI (below). In the present report, we extend our studies on MLRI as well as introduce a new asymmetric glycerol-based lipid, PMD1.

It has been our observation, as well as that of others,[15] that, of the structural variables listed above, chain length is the strongest contributor to transfection efficacy. Indeed, Koynova et al. recently noted in a detailed study of *O*-alkyl phosphatidylcholinium derivatives that the hydrocarbon chain variations of these cationic lipids modulated by over 2 orders of magnitude their transfection activity.[27] The type of chemical linker, and to a lesser extent the headgroup, seem to have the strongest contribution to toxicity.[28,29] But for any comparison of otherwise identical and optimized lipids,

(7) Niculescu-Duvaz, D.; Heyes, J.; Springer, C. J. Structure-activity relationship in cationic lipid mediated gene transfection. *Curr. Med. Chem.* **2003**, *10* (14), 1233–1261.
(8) Ewert, K. K.; Evans, H. M.; Ahmad, A.; Slack, N. L.; Lin, A. J.; Martin-Herranz, A.; Safinya, C. R. Lipoplex structures and their distinct cellular pathways. *Adv. Genet.* **2005**, 53PA 119–155.
(9) Bennett, M. J.; Aberle, A. M.; Balasubramaniam, R. P.; Malone, J. G.; Malone, R. W.; Nantz, M. H. Cationic lipid-mediated gene delivery to murine lung:correlation of lipid hydration with in vivo transfection activity. *J. Med. Chem.* **1997**, *40*, 4069–4078.
(10) Nantz, M. H.; Li, L.; Zhu, J.; Aho-Sharon, K. L.; Erickson, K. L. Inductive electron-withdrawal from ammonium ion headgroups of cationic lipids and the influence on DNA transfection. *Biochim. Biophys. Acta* **1998**, *1394* (2−3), 219–223.
(11) Srilakshmi, G. V.; Sen, J.; Chadhuri, A.; Ramadas, Y.; Rao, N. M. Anchor-dependent lipofection with non-glycerol based cytofectins containing single 2-hydroxyethyl head groups. *Biochim. Biophys. Acta* **2002**, *1559*, 8795.
(12) Hattori, Y.; Ding, W.-X.; Maitani, Y. Highly efficient cationic hydroxyethylated cholesterol-based nanoparticle-mediated gene transfer in vivo and in vitro in prostate carcinoma PC-3 cells. *J. Controlled Release* **2007**, *120*, 1221–1230.
(13) Yingyongnarongkul, B.; Radchatawedchakoon, W.; Krajarng, A.; Watanapokasin, R.; Suksamrarn, A. High transfection efficiency and low toxicity cationic lipids with aminoglyceroldiamine conjugate. *Bioorg. Med. Chem.* **2009**, *17*, 176188.
(14) Balasubramaniam, R. P.; Bennett, M. J.; Aberle, A. M.; Malone, J. G.; Nantz, M. H.; Malone, R. W. Structural and functional analysis of cationic transfection lipids: The hydrophobic domain. *Gene Ther.* **1996**, *3*, 163–172.
(15) Kim, H. S.; Moon, J.; Kim, K. S.; Choi, M. M.; Lee, J. E.; Heo, Y.; Cho, D. H.; Jang, D. C.; Park, Y. S. Gene-Transferring Efficiencies of Novel Diamino Cationic Lipids with Varied Hydrocarbon Chains. *Bioconjugate Chem.* **2004**, *15*, 1095–1101.
(16) Rajesh, M.; Sen, J.; Srujan, M.; Mukherjee, K.; Sreedhar, B.; Chaudhuri, A. Dramatic influence of the orientation of linker between hydrophilic and hydrophobic lipid moiety in liposomal gene delivery. *J. Am. Chem. Soc.* **2007**, *129*, 11408–11420.
(17) Chen, H.; Zhang, H.; McCallum, C. M.; Szoka, F. C. Unsaturated cationic ortho esters for endosome permeation in gene delivery. *J. Med. Chem.* **2007**, *50*, 4269–4278.
(18) Byk, G.; Dubertret, C.; Escriou, V.; Frederic, M.; Jaslin, G.; Rangara, R.; Pitard, B.; Crouzet, J.; Wils, P.; Schwartz, B.; Scherman, D. Synthesis, Activity, and Structure-Activity Relationship Studies of Novel Cationic Lipids for DNA Transfer. *J. Med. Chem.* **1998**, *41*, 224–235.
(19) Savva, M.; Chen, P.; Aljaberi, A.; Selvi, B.; Spelios, M. In Vitro Lipofection with Novel Asymmetric Series of 1,2-Dialkoylamidopropane-Based Cytofectins Containing Single Symmetric Bis-(2-dimethylaminoethane) Polar Headgroups. *Bioconjugate Chem.* **2006**, *16*, 1411–1422.
(20) Liu, D.; Qiao, W.; Li, Z.; Chen, Y.; Cui, X.; Li, K.; Yan, K.; Zhu, L.; Guo, Y.; Cheng, L. Structure-Function Relationship Research of Glycerol Backbone-Based Cationic Lipids for Gene Delivery. *Chem. Biol. Drug Des.* **2008**, *71*, 336–344.
(21) Aberle, A. H.; Bennett, M. J.; Malone, R. W.; Nantz, M. H. The counterion influence on cationic lipid-mediated transfection of plasmid DNA. *Biochim. Biophys. Acta* **1996**, *1299*, 281–283.
(22) Reynier, P.; Briane, D.; Coudert, R.; Fadda, G.; Bouchemal, N.; Bissieres, P.; Taillandier, E.; Cao, A. Modifications in the head group and in the spacer of cholesterol-based cationic lipids promote transfection in melanoma B16-F10 cells and tumours. *J. Drug Targeting* **2004**, *12* (1), 25–38.
(23) Lin, A. J.; Slack, N. L.; Ahmad, A.; George, C. X.; Samuel, C. E.; Safinya, C. R. Three-dimensional imaging of lipid gene-carriers: membrane charge density controls universal transfection behavior in lamellar liposome-DNA complexes. *Biophys. J.* **2003**, *84* (5), 3307–3316.
(24) Masotti, A.; Mossa, G.; Cametti, C.; Ortaggi, G.; Bianco, A.; Grosso, N. D.; Malizia, D.; Esposito, C. Comparison of different commercially available cationic liposome-DNA lipoplexes: Parameters influencing toxicity and transfection efficiency. *Colloids Surf., B* **2009**, *68* (2), 136–144.
(25) Santel, A.; Aleku, M.; Keil, O.; Endruschat, J.; Esche, V.; Fisch, G.; Dames, S.; Laffler, K.; Fechtner, M.; Arnold, W.; Giese, K.; Klippel, A.; Kaufman, J. A novel siRNA-lipoplex technology for RNA interference in the mouse vascular endothelium. *Gene Ther.* **2006**, *13*, 1222–1234.
(26) Majeti, B. R.; Singh, R. S.; Yadav, S. K.; Bathula, S. R.; Ramakrishna, S.; Diwan, P. V.; Madhavendra, S. S.; Chaudhuri, A. Enhanced Intravenous Transgene Expression in Mouse Lung Using Cyclic-Head Cationic Lipids. *Chem. Biol.* **2004**, *11*, 427–437.

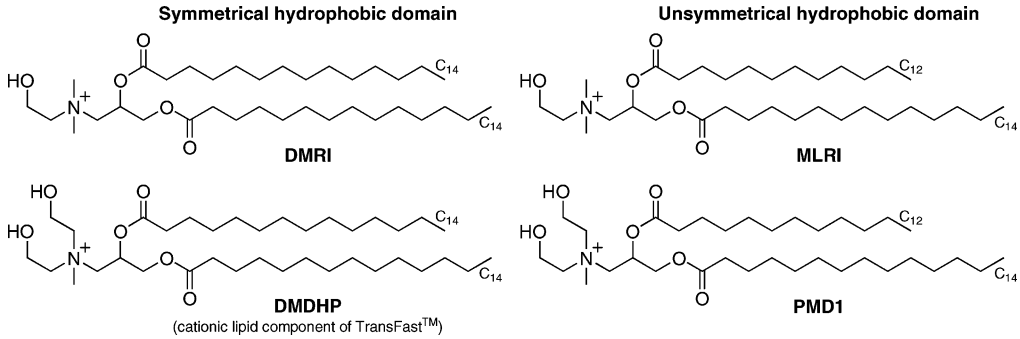

Figure 2. Comparison of hydrophobic domain composition.

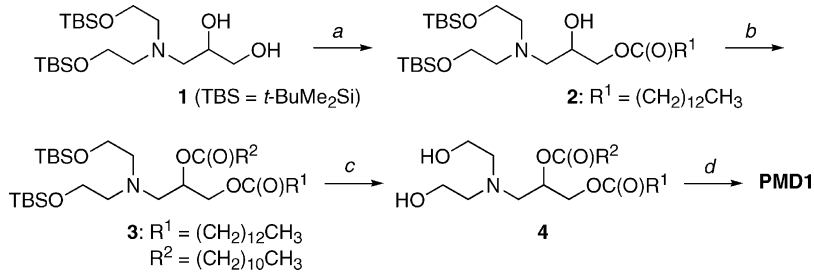

Figure 3. PMD1 synthesis. Legend: (a) myristic anhydride (1.0 equiv), Et_3N (2 equiv), DMAP (0.05 equiv), CH_2Cl_2, 0 °C, 4 h, 80%; (b) lauric anhydride (1.2 equiv), Et_3N (2 equiv), DMAP (0.05 equiv), CH_2Cl_2, rt, 12 h, 98%; (c) TBAF (3 equiv), THF, 0 °C to rt, 2 h, 91%; (d) MeI (excess), 50 °C, 61%.

asymmetric chains perform better at transfection than symmetric hydrocarbons. We hypothesize that this effect is due to biological membrane fluidity effects of optimally sized but asymmetric hydrocarbon chains.

After extensive comparisons *in vitro* with commercially available transfection lipids (not reported), we selected MLRI for further studies. We have previously reported excellent transfection results *in vivo* with MLRI (Figure 2),[30−32] an asymmetric C(14)−C(12) cationic lipid variant of the highly active C(14)−C(14) cationic lipid DMRI.[6] By analogy, we postulated that an unsymmetrical analogue of DMDHP (Figure 2) might also exhibit higher activity than its symmetrical counterpart, thus further optimizing overall transfection.[33,34] Consequently, we report herein the synthesis of PMD1 (Figure 3) and our observations on the influence of hydrophobic domain asymmetry in the transfection of mouse CNS. We compared a series of lipids that vary only in hydrocarbon asymmetry using whole animal brain imaging.

Methods

Chemistry. For this report, two custom cationic lipids, MLRI and PMD1 (Figure 2), were compared with the commercially available transfection reagents DOTAP (Avanti Polar Lipids, Alabaster, AL), TransFast (Promega Corporation, Madison, WI) and Lipofectamine (Invitrogen, Carlsbad, CA).

These lipids were selected for similarities and differences in the lipid structure variables that we wished to compare. For instance, TransFast, which is composed of the synthetic cationic lipid {bis (2-hydroxyethyl)}-*N*-methyl-*N*-{2,3-di(tetradecanoyloxy)propyl} ammonium iodide (DMDHP, Figure 2) and the neutral lipid dioleoylphosphatidylethanolamine (DOPE), is a symmetrical analogue of PMD1. DOTAP and Lipofectamine are also among the most commonly used reagents for transfection applications, and thus serve as

(27) Koynova, R.; Tenchov, B.; Wang, L.; MacDonald, R. C. Hydrophobic moiety of cationic lipids strongly modulates their transfection activity. *Mol. Pharmaceutics* **2009**, *6*, 951–958.
(28) Aberle, A. M.; Tablin, F.; Zhu, J.; Walker, N. J.; Gruenert, D. C.; Nantz, M. H. A novel tetraester construct that reduces cationic lipid-associated cytotoxicity. Implications for the onset of cytotoxicity. *Biochemistry* **1998**, *37*, 6533–6540.
(29) Leventis, R.; Silvius, J. R. Interactions of mammalian cells with lipid dispersions containing novel metabolizable cationic amphiphiles. *Biochim. Biophys. Acta* **1990**, *1023* (1), 124–132.
(30) Hecker, J. G.; Hall, L. L.; Irion, V. R. Non-viral gene delivery to the lateral ventricles in rat brain: initial evidence for widespread distribution and expression in the central nervous system. *Mol. Ther.* **2001**, *3* (3), 375–384.
(31) Anderson, D. M.; Hall, L. L.; Ayyalapu, A.; Irion, V. R.; Nantz, M. H.; Hecker, J. G. Stability of mRNA/cationic lipid lipoplexes in human and rat cerebrospinal fluid: methods and evidence for non-viral mRNA gene delivery to the CNS. *Hum. Gene Ther.* **2003**, *14* (3), 191–202.
(32) Hauck, E. S.; Zou, S.; Scarfo, K. A.; Nantz, M. H.; Hecker, J. G. Whole animal in vivo imaging after transient non-viral lipid-mediated gene transfer to the rat central nervous system. *Mol. Ther.* **2008**, *16* (11), 1857–1864.
(33) Oler, J.; Schenborn, E. TransFast transfection reagent update. *Promega Notes* **1999**, *17*, 18–23.
(34) Ango, F.; Albani-Torregrossa, S.; Joly, C.; Robbe, D.; Michel, J. M.; Pin, J. P.; Bockaert, J.; Fagni, L. A simple method to transfer plasmid DNA into primary cultures: functional expression of the mGlu5 receptor in cerebellar granule cells. *Neuropharmacology* **1999**, *38* (6), 793–803.

positive controls for comparison purposes. MLRI has been previously reported,[14] and PMD1 was prepared as outlined in Figure 3 from known aminodiol **1**.[35]

3-(Bis-{2-(*tert*-butyldimethylsilyloxy)ethyl}amino)propane-1,2-diol (2). To a solution of diol **1** (165 mg, 0.405 mmol) in CH_2Cl_2 (2 mL) were added triethylamine (0.11 mL, 0.81 mmol) and DMAP (2 mg). The reaction mixture was cooled to 0 °C, and myristic anhydride (187 mg, 0.405 mmol) was added. The reaction was stirred at 0 °C for 4 h and then poured over saturated aqueous $NaHCO_3$. The aqueous layer was extracted with CH_2Cl_2, and the combined organic layer was washed with water and brine, dried (Na_2SO_4), and then concentrated by rotary evaporation. The residue was purified by column chromatography (SiO_2; 4:1, hexane:ethyl acetate) to give monoester **2** as a colorless oil (200 mg, 80%): ^{1}H NMR ($CDCl_3$) δ 0.06 (s, 12H), 0.89 (m, 21H), 1.25 (m, 20H), 1.62 (m, 2H), 2.33 (t, J = 7.5 Hz, 2H), 2.53 (dd, J = 12.9, 9.9 Hz, 1H), 2.73 (dd, J = 12.9, 3.6 Hz, 1H), 2.76 (t, J = 5.7 Hz, 4H), 3.65−3.70 (m, 4H), 3.78−3.86 (m, 1H), 4.00 (dd, J = 11.4, 6.0 Hz, 1H), 4.12 (dd, J = 11.4, 4.2 Hz, 1H); ^{13}C NMR ($CDCl_3$) δ −5.4, 14.1, 18.3, 22.7, 24.8, 24.9, 25.9, 29.1, 29.2, 29.3, 29.5, 29.6, 29.6, 29.7, 31.9, 34.2, 57.1, 58.0, 61.5, 66.2, 66.4, 173.9.

3-{Bis{2-(*tert*-butyldimethylsilyloxy)ethyl}amino}-2-dodecanoyloxy-1-tetradecanoyloxy-propane (3). To a solution of ester **2** (200 mg, 0.324 mmol) in CH_2Cl_2 were added triethylamine (90 μL, 0.648 mmol) and DMAP (2 mg). The mixture was cooled to 0 °C, and lauric anhydride (152 mg, 0.389 mmol) was added. The reaction mixture was stirred for 18 h at rt, then poured over saturated aqueous $NaHCO_3$, and extracted with CH_2Cl_2. The combined organic layer was washed with water and brine, dried (Na_2SO_4), and concentrated. The residue was chromatographed (SiO_2; 9:1, hexane: ethyl acetate) to afford diester **3** as a colorless oil (255 mg, 98%): ^{1}H NMR ($CDCl_3$) δ 0.05 (s, 12H), 0.88 (m, 24H), 1.25 (m, 36H), 1.56−1.68 (m, 4H), 2.28 (t, J = 7.5 Hz, 2H), 2.29 (t, J = 7.5 Hz, 2H), 2.67−2.74 (m, 6H), 3.63 (t, J = 6.6 Hz, 4H), 4.12 (dd, J = 12.0, 6.0 Hz, 1H), 4.36 (dd, 12.0, 3.0 Hz, 1H), 5.08 (m, 1H); ^{13}C NMR ($CDCl_3$) δ −5.4, 14.1 (2C), 18.2, 22.7 (2C), 24.9 (2C), 25.9, 29.1 (2C), 29.3 (2C), 29.4 (2C), 29.5 (2C), 29.6−29.7 (6C), 31.9 (2C), 34.2, 34.4, 55.6, 57.6, 61.9, 63.6, 70.1, 173.1, 173.5.

3-{Bis(2-hydroxyethyl)amino}-2-dodecanoyloxy-1-tetradecanoyloxypropane (4). To a solution of diester 3 (255 mg, 0.318 mmol) in THF (2 mL) at 0 °C was added a solution of tetra-*n*-butylammonium fluoride (0.95 mL of a 1.0 M solution in THF, 0.95 mmol). The reaction mixture was stirred for 2 h, warmed to rt, and then poured over saturated aqueous $NaHCO_3$ and extracted with ether. The combined organic layer was washed with water and brine, dried (Na_2SO_4), and concentrated by rotary evaporation. The residue was purified by column chromatography (SiO_2; 1:1, hexane:ethyl acetate) to provide diol **4** as a white solid (165 mg, 91%): ^{1}H NMR ($CDCl_3$) δ 0.88 (m, 6H), 1.25 (m, 36H), 1.61 (m, 4H), 2.31 (t, J = 7.2 Hz, 2H), 2.34 (t, J = 7.2 Hz, 2H), 2.68−2.74 (m, 6H), 3.61 (t, J = 5.4 Hz, 4H), 4.11 (dd, J = 12.0, 6.0 Hz, 1H), 4.36 (dd, J = 12.0, 3.6 Hz, 1H), 5.19 (m, 1H); ^{13}C NMR ($CDCl_3$) δ 14.1 (2C), 22.7 (2C), 24.9 (2C), 29.1 (2C), 29.3 (2C), 29.4 (2C), 29.5 (2C), 29.6−29.7 (6C), 31.9 (2C), 34.1, 34.4, 56.0, 57.2, 59.9, 63.5, 70.1, 173.6, 174.0.

(2-Dodecanoyloxy-3-tetradecanoyloxypropyl)-bis(2-hydroxyethyl)methane-ammonium iodide (PMD1). A 10 mL flask fitted with a reflux condenser was charged with methyl iodide (3 mL) and diester **4** (165 mg, 0.288 mmol). {Note: methyl iodide was pretreated by passing through a small pipet containing neutral alumina.} The reaction mixture was heated at 50 °C for 18 h whereupon the methyl iodide then was removed using a steady stream of argon. The crude residue was purified by column chromatography (SiO_2; 9:1, CH_2Cl_2: MeOH) to give PMD1 as a white solid (125 mg, 61%): ^{1}H NMR ($CDCl_3$) δ 0.88 (m, 6H), 1.25 (m, 36H), 1.61 (m, 4H), 2.34 (t, J = 7.5 Hz, 2H), 2.37 (t, J = 7.5 Hz, 2H), 3.38 (s, 3H), 3.79−3.84 (m, 1H), 3.80−3.95 (m, 4H), 4.00−4.06 (m, 1H), 4.11 (dd, J = 12.0, 6.0 Hz, 1H), 4.15−4.18 (m, 1H), 4.22−4.29 (m, 3H), 4.48 (dd, J = 12.0, 3.6 Hz, 1H), 5.71 (m, 1H); ^{13}C NMR ($CDCl_3$) δ 14.1 (2C), 22.7 (2C), 24.6, 24.7, 29.1 (2C), 29.3 (12C), 31.9 (2C), 34.0, 34.3, 51.3, 55.7, 63.3, 64.0, 65.0, 65.5, 172.8, 173.3. HRMS $[M - I]^+$: calcd 586.5047, found 586.5045.

Lipids and Formulation of Lipid:Nucleic Acid Complexes (Lipoplexes). MLRI, PMDI and DOTAP were prepared by supplementation with DOPE in chloroform in a 1:1 molar ratio. Lipofectamine and TransFast were used as supplied by the manufacturer and optimized *in vitro* in CHO and NIH3T3 cells, as were all lipids (not reported here). DNA/lipid complexes were formed by combining the described lipid preparation with plasmid DNA expressing luciferase and previously described in a previously determined optimal charge ratio of 3:1 lipid-to-nucleic acid for MLRI,[30,31] TransFast, and DOTAP, while optimal ratios for PMD1 and Lipofectamine were 1:1 and 2:1, respectively. Mixtures for *in vivo* experiments were adjusted to 10 μL containing 3 μg of pND.luciferase DNA and proportionate amount of lipid constituted in OptiMem (Invitrogen, Carlsbad, CA). Mixtures were incubated at 37 °C for 30 min before delivery *in vivo*.

***In Vivo* Delivery.** 40 C57/B16 mice from Charles River (Horsham, PA) were randomly divided into five groups of 8 mice each for each lipid. For DNA lipoplex injection animals were first anesthetized with ketamine/Xylazine ip. After sterile prep 10 μL of previously prepared lipoplexes was delivered into cisterna magna by slow injection via using a 24-gauge Hamilton syringe. Live anesthetized animals were imaged for luciferase activity 48 h after injection, which we have previously shown to correspond to the peak in luciferase transfection expression.[32] For imaging, animals were first injected via tail vein with luciferin, then quickly anesthetized with an ip injection of 200 μL of ketamine/xylazine (100 mg/kg, 20 mg/kg).

(35) Nantz, M. H.; Bennett, M. J.; Balasubramaniam, R. P. Polyfunctional Cationic Cytofectins; U.S. Patent No. 5,869,715, 1999.

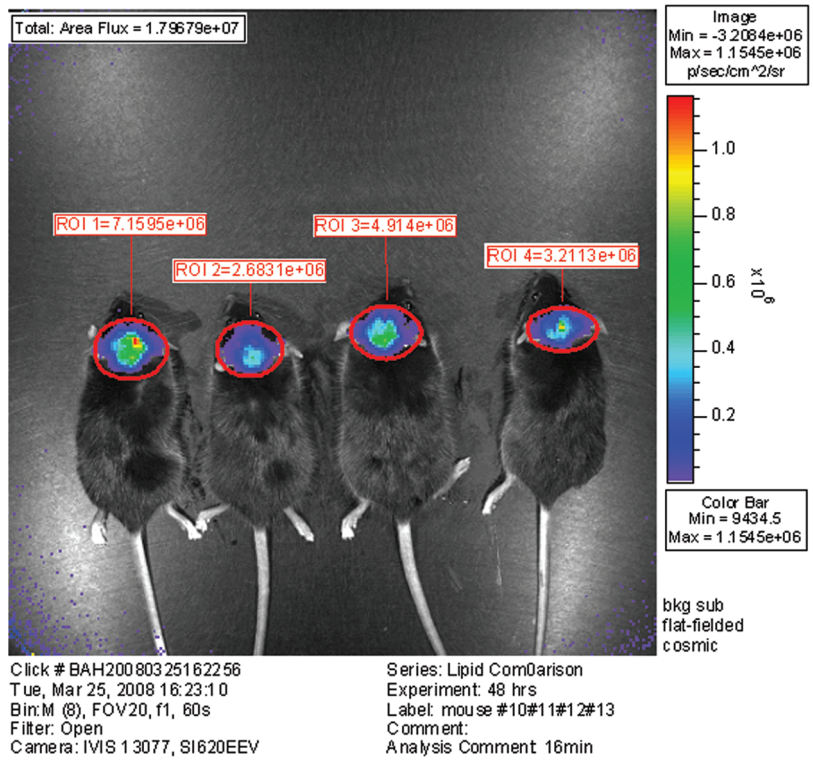

Figure 4. Example of *in vivo* imaging of multiple mice after lipid/DNA lipoplex delivery to mouse brain. 48 h after a single injection of DNA/lipid lipoplex, in this case lipid PMD1, encoding for luciferase, animals were anesthetized, intravenous catheters were placed, and luciferin was injected. Photons (RLUs) were accumulated in timed fashion.

***In Vivo* luciferase imaging.** A Xenogen IVIS 100 was used to image the animals after vector delivery. Luciferin was injected iv and luciferase activity followed over time by light emission detection. After animals were anesthetized, they were quickly placed in groups in the light tight imaging box. A light image (photograph) of the animal was taken, and then a background image of the photons of emitted light was collected by the cooled charge-coupled device camera of the IVIS 100 system over a period of 1 min using medium binning. Our data acquisition time was chosen based on reported experiments that used mice as animal models for *in vivo* imaging, which ranged from 10 s to 2 min, adjusted so as to avoid pixel saturation. 150 mg/kg of luciferin was our chosen initial dose of substrate as it is recommended by Xenogen and is also the most common dose reported in the literature, albeit for intraperitoneal injection. We varied luciferin dose in additional experiments, not reported here, to arrive at a balance between luciferase signal, luciferin expense, and luciferin buffer salt load to the animals. We found that the above dose of the luciferin was optimal, but that the substrate needed to be dissolved in sterile water to avoid delivering a salt load to the animal that could be fatal.

The peak and duration of luciferase activity after iv injection of luciferin were determined by IVIS imaging of animals every 1−2 min, with a constant image acquisition time of 1 min, until a clear peak of light emission was detected or until the signal decreased to less than 20% of peak. The time we expected for peak luciferase activity was determined previously.[32,36] Using the Living Image software (Xenogen), ROIs were created over areas of intense light emission and the photons emitted at each time point were quantified. Because there was some variability in the time of peak luciferase activity, multiple IVIS images were taken after each iv luciferin injection in all experiments. *In vivo* images of groups of mice were collected at 2−4 min intervals for approximately 30 min, and time after injection of luciferin was carefully calculated for each animal. Anatomical localization was obtained by the superposition of the luminescent image over the light image (example is shown in Figure 4). Each image (i.e., time point) is thus a composite of a photograph of the animal and the acquired luminescent image. ROIs were created using LivingImage software (Xenogen) on a computer that was dedicated to the IVIS system for data acquisition. These ROIs identify the location of the most intense signal in the CNS after delivery of the substrate.

Results

The results of *in vivo* imaging of whole animals 48 h after intrathecal injection of a lipid-mediated DNA lipoplex encoding for luciferase show clear advantages in expression

(36) Yellayi, S.; Ghazanfar, M.; Xu, H. W.; Weber, M.; Hecker, J. G.; Tone, M.; Tsingalia, A.; Tymianski, M. A. A combination of delayed type-hypersensitivity and gene transfer to screen novel immunosuppressive molecules. *Mol. Ther.*, submitted.

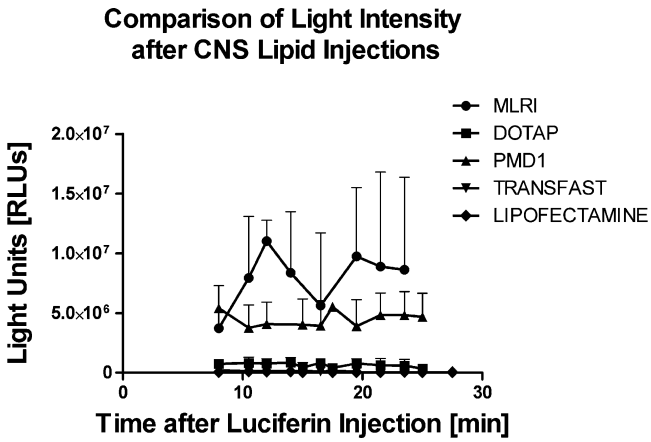

Figure 5. Comparison of simultaneous *in vivo* gene delivery to cisterna magna of DNA luciferase for a series of matched asymmetric and symmetric dual chain glycerol-based lipids. Groups of $N = 8$ mice were injected with a series of DNA/cationic lipid lipoplexes that had been previously optimized for each lipid individually for charge ratio and incubation time. 48 h later each mouse was anesthetized and luciferin, the luciferase substrate, was injected intravenously in the tail vein. *In vivo* images of groups of mice were collected at 2−4 min intervals for approximately 30 min.

of MLRI and PMD1 lipids. Figure 4 is an example of *in vivo* imaging of multiple mice 48 h after a single injection of lipid/DNA lipoplex encoding for luciferase to mouse brain. Figure 5 shows averaged results over time for each of the lipids, with error bars showing standard deviation for each average. Number of measurements for each lipid at each time point varied from 2 to 7, due to the logistical challenges of anesthetizing, placing intravenous catheters, injecting luciferin, and simultaneously imaging 3−5 mice at a time. In contrast to our results with luciferase expressing DNA lipoplexes injected into rat lateral ventricle or cisterna magna, we were not always able to readily identify a peak in expression over time. To illustrate the differences in expression in another way we also tabulated the results for each lipid ($N = 33$ (MLRI) to 54 (PMD1)) and analyzed the RLU photon counts for each lipid. Both asymmetric lipids, MLRI and PMD1, are markedly more efficient at transfecting mouse brain. These averages and standard deviations are shown in Figure 6.

Statistical Methods

Since several *in vivo* measurements were obtained from each mouse, a repeated measures analysis of variance (ANOVA) was used to evaluate the association between the type of lipid and the *in vivo* measurements. Results were analyzed using a one-way ANOVA followed by Tukey's multiple comparison test. Results are reported as significant ($P < 0.05$, *) and highly significant ($P < 0.01$), ***). All statistical analyses were conducted using SAS v.9.2 (SAS Institute, Inc., Cary, NC) and R v2.7.2 (The R Foundation for Statistical Computing, Vienna, Austria).

Statistical Results

Figure 6 shows the overall lipid means. In this figure, the 25th percentile, median, and 75th percentile are represented with the bottom, middle, and top lines of each box; the mean and 95% confidence intervals of the mean are depicted with the diamond and arrows inside each box. Measurements associated with MLRI and PMDI tend to be much higher than those obtained with the other three lipids.

Tables 1 and 2 summarize the analysis results. These results indicate a highly significant association between lipid type and the *in vivo* measurements ($p = 0.0008$), with MLRI and PMDI lipids yielding the highest outcome measurements.

Table 2 displays pairwise differences between least-squares (i.e., ANOVA adjusted) lipid means. At a Bonferroni-adjusted significance level of 0.005, we note that all pairwise differences except the LIPOF/TRANSF and MLRI/PMDI differences are statistically significant.

Discussion

The present work describes the first examples of asymmetric glycerol-based lipids for *in vivo* transfection and a comparison to symmetric analogues using whole animal *in vivo* imaging. There are several comparisons of transfection efficacy between asymmetric lipids and their symmetric counterparts in the literature; however, these studies are principally relegated to *in vitro* transfections, as summarized in Table 3. In addition to the *in vitro* results described, we located two reports on *in vivo* comparison of asymmetric dual-chain cationic lipids, in mouse endothelium and lung, respectively.[25,26] Whereas these lipids are not glycerol-based lipids and do not target the CNS, we include these for discussion and because these are the only other *in vivo* examples we can find that investigate hydrophobic domain asymmetry in any way.

Our experiments and resulting observations (and literature summary) deal with dual-chain, cationic lipids, of which the glycerol based are by far the most frequently used and reported. Few dual-chain, cationic lipids possessing unsymmetrical hydrophobic domains have been reported,[14,25,37−40] and it is the additional synthetic challenge of differentiating lipid side chains that is likely responsible for this sparse

(37) Heyes, J. A.; Niculescu-Duvaz, D.; Cooper, R. G.; Springer, C. J. Synthesis of novel cationic lipids: effect of structural modification on the efficiency of gene transfer. *J. Med. Chem.* **2002**, *45* (1), 99–114.

(38) Dileep, P. V.; Antony, A.; Bhattacharya, S. Incorporation of oxyethylene units between hydrocarbon chain and pseudoglyceryl backbone in cationic lipid potentiates gene transfection efficiency in the presence of serum. *FEBS Lett.* **2001**, *509*, 327–331.

(39) van der Woude, I.; Wagenaar, A.; Meekel, A. A. P.; Ter Beest, M. B. A.; Ruiters, M. H. J.; Engberts, J. B. F. N.; Hoekstra, D. Novel pyridinium surfactants for efficient, nontoxic in vitro gene delivery. *Proc. Natl. Acad. Sci. U.S.A.* **1997**, *94*, 1160–1165.

(40) Banerjee, R.; Das, P. K.; Srilakshmi, G. V.; Chaudhuri, A.; Rao, N. M. Novel series of non-glycerol-based cationic transfection lipids for use in liposomal gene delivery. *J. Med. Chem.* **1999**, *42* (21), 4292–4299.

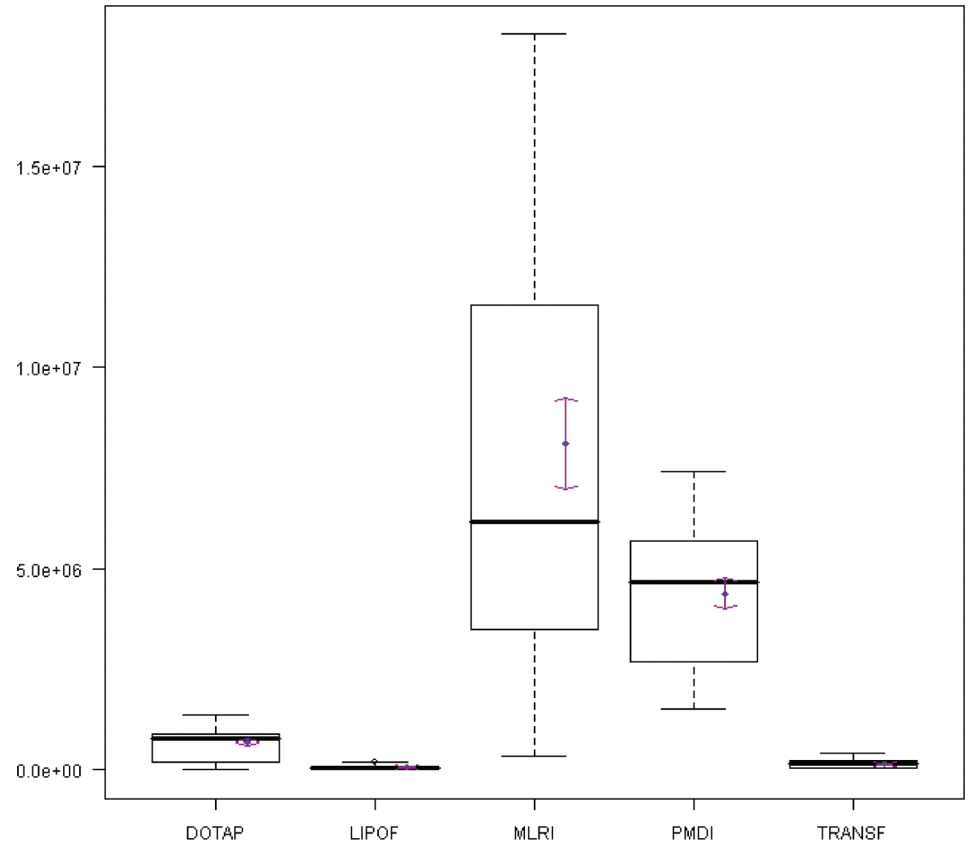

Figure 6. Averaged measurements for all lipids. Results for all measurements for all animals for each of the lipids were tabulated. Average and standard deviation were calculated for each lipid. Statistics for these results are shown in Tables 1 and 2, which are graphically depicted in Figure 6. In this figure, the 25th percentile, median, and 75th percentile are represented with the bottom, middle, and top lines of each box; the mean and 95% confidence intervals of the mean are depicted with the diamond and arrows inside each box. Measurements associated with MLRI and PMDI are much higher than those obtained with the other three lipids.

Table 1. Repeated Measures ANOVA Results

source	DF	chi-square	Pr > ChiSq
lipid	4	18.92	0.0008

Table 2. Differences in Least Squares Means

lipid 1	lipid 2	chi-square	*P* value
DOTAP	LIPOF	19.03	<0.0001
DOTAP	MLRI	16.32	<0.0001
DOTAP	PMDI	31.84	<0.0001
DOTAP	TRANSF	13.94	0.0002
LIPOF	MLRI	19.32	<0.0001
LIPOF	PMDI	45.7	<0.0001
LIPOF	TRANSF	3.81	0.0511
MLRI	PMDI	3.68	0.0551
MLRI	TRANSF	18.93	<0.0001
PMDI	TRANSF	43.94	<0.0001

representation.[41,42] Furthermore, to our knowledge, there are no commercial sources of transfection lipids of this type. Consequently, limited data are available regarding the influence of hydrophobic domain asymmetry on transfection activity. Since the initial observation that hydrophobic domain asymmetry is beneficial,[14] several groups have examined unsymmetrical lipids in gene transfer experiments *in vitro*. With remarkable agreement, the reported unsymmetrical lipids have shown higher transfection efficiencies than symmetrical counterparts (Table 3).[7] This consistent structure−activity relationship does not appear to be dependent on the nature of the DNA-binding domain. Indeed, the polar domains of these unsymmetrical lipids feature charged nitrogen in the form of pyridinium (SAINT-8, Table 3), nonquaternary ammonium (lipid **37**, Table 3), and quaternary ammonium, either as a nonfunctionalized (lipid **3**, Table 3) or 2-hydroxyethyl-functionalized (MLRI, MOOHAC in Table 3, or PMD1) salt. The hydrophobic domain asymmetry in these examples also is not restricted to differences in side chain lengths. As seen with lipids SAINT-8 (Table 3) and MOOHAC (Table 3), a difference in side chain unsaturation is also a feature that improved the transfection activity. The results herein using PMD1 in comparison to its symmetrical analogue DMDHP are consistent with this observation; namely, subtle changes in the hydrophobic domain composition that introduce asymmetry, sometimes as slight as a two-carbon chain length difference, are sufficient to improve the gene transfer activity.

The mechanism whereby hydrophobic domain asymmetry influences the transfection activity of a given lipid is a

Table 3. Examples of Unsymmetrical Dual-Chain Cationic Lipids That Have Higher *in Vitro* Transfection Efficiencies in Comparison to Corresponding Symmetrical Analogues

Unsymmetrical hydrophobic domain	Symm. analog(s)	Cell line (charge ratio if available)	Ref.
A. Glycerol based lipids			
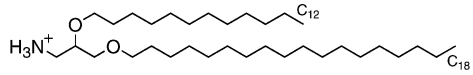 lipid **37**	C_{18}, C_{18}	V79 (3:1)[a]	Heyes [37]
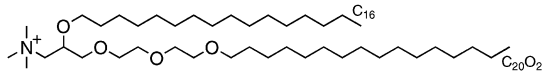 lipid **3**	C_{16}, C_{16}	HeLa (1:1)[b]	Dileep [38]
B. Non-glycerol based lipids			
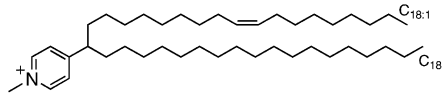 **SAINT-8**	C_{18}, C_{18}	COS-7[b]	van der Woude [39]
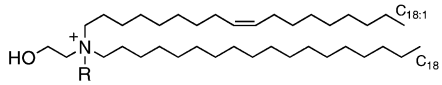 R = CH_3, **MOOHAC**	C_{18}, C_{18}	COS-1 (0.1:1)[c]	Banerjee [40]
R = CH_3CH_2OH, lipid **13**	C_{18}, C_{18}, $C_{18:1}$,$C_{18:1}$	CHO (1:1)[c]	Singh [51]
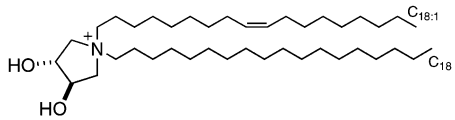 lipid **4**	C_{18}, C_{18}	COS-1 (0.3:1)[c] CHO (0.3:1)[c] HepG2 (0.3:1)[c]	Majeti [26]

[a] these cationic lipids were co-formulated with DC-Chol and DOPE; [b] co-formulated with DOPE; [c] co-formulated with cholesterol.

complex issue and likely is a combination of influences exerted at different stages along the transfection path. One possible explanation for these observations, as initially suggested by Springer et al.,[37] is that the asymmetry affects both derived lipoplex fluidity and stability, and that the changes in these properties, in turn, improve lipoplex fusogenicity.

Another consideration that has received recent attention is the intrinsic asymmetry of *lipoplex* preparations. In an elegant study on the self-assembly process of DNA lipoplex formation, MacDonald[43] notes the heterogeneity within lipoplex particles. Certainly lipid asymmetry can be expected to contribute to overall liposome heterogeneity, which, in turn, may lead to different percentages of subpopulations, potentially favoring the postulated transfection-active multilamellar lipoplex subset. In addition there are multiple ways that lipoplex domains are affected, even as nucleic acids condense and form heterogeneous complexes.

Fusogenic events between lipoplex formulations and the plasma membrane, as well as the endosomal membrane, are key determinants of transfection activity.[44−47] In cases where the hydrophobic domain is composed of chains

(41) Guivisdalsky, P. N.; Bittman, R. Regiospecific opening of glycidyl derivatives mediated by boron trifluoride. Asymmetric synthesis of ether-linked phospholipids. *J. Org. Chem.* **1989**, *54*, 4637–4642.

(42) Bennett, M. J.; Malone, R. W.; Nantz, M. H. A flexible approach to synthetic lipid ammonium salts for polynucleotide transfection. *Tetrahedron Lett.* **1995**, *36*, 2207–2210.

(43) Pozharski, E. V.; MacDonald, R. C. Single lipoplex study of cationic lipoid-DNA self-assembled complexes. *Mol. Pharmaceutics* **2007**, *4*, 962–974.

(44) Duzgunes, N.; Goldstein, J. A.; Friend, D. S.; Felgner, P. L. Fusion of liposomes containing a novel cationic lipid, N-[2,3-(dioleyloxy)propyl]-N, N, N-trimethylammonium: induction by multivalent anions and asymmetric fusion with acidic phospholipid vesicles. *Biochemistry* **1989**, *28*, 9179–9184.

(45) Ramezani, M.; Khoshhamdam, M.; Dehshahri, A.; Malaekeh-Nikouei, B. The influence of size, lipid composition and bilayer fluidity of cationic lipids on the transfection efficiency of nanolipoplexes. *Colloids Surf., B* **2009**, *72* (1), 1–5.

(46) Ma, B.; Zhang, S.; Jiang, H.; Zhao, B.; Lv, H. Lipoplex morphologies and their influences on transfection efficiency in gene delivery. *J. Controlled Release* **2007**, *123* (3), 184–194.

having different lengths, as with PMD1 and MLRI, the asymmetry weakens the intermolecular lateral interactions between adjacent lipids in a bilayer, imparting as much as 20−25% greater in-plane elasticity than corresponding symmetrical analogues.[48] The greater fluidity is a consequence of several factors, such as (a) the decrease in surrounding hydrocarbon contacts for the longer chains, (b) the void spaces created by the decreased packing density of the shorter chains, and (c) the disruption of van der Waals packing interactions by the terminal methyl groups of the shorter chains, which have a larger effective volume as compared to that of a methylene group. Mui et al. state that membrane perturbations are key for transfection, and report that their measurements using DOPE suggest that the asymmetric lipids help with lipoplex uptake in a similar mechanism.[49,50] Due to mismatch in the chain lengths and chain backbone linkage region of lipid **3** (Table 3), this lipid would assemble in a rather disorganized manner in its membranous aggregate, and such local disorders in the cell membrane might account for the efficient delivery of the DNA inside the cell.[49] This suggests that the lipids must perturb the membrane for efficient transfection to occur, and the asymmetry helps to do this.

Fusogenicity (therefore) appears to be greatly influenced by altering side chain lengths. We believe that transfection activity and efficacy is largely due to headgroup and side chain composition, although charge ratio, nucleic acid condensation, presence of unsaturations, and lamellar microstructures are also important. If the side chain length of one chain is now varied, liposome (and derived lipoplex) stability is decreased because the packing forces are not as strong for mismatched domains. This affects fusogenicity and likely also lipoplex disassembly, another key step in the transfection process. If one optimizes headgroup and side chain composition and identifies an "optimal" lipid for a particular cell type, we predict that an asymmetric variant of that lipid will be even more active. Thus, when optimizing a transfection lipid consider altering the hydrocarbon domain symmetry. We found that MLRI is very efficient at transfecting a wide variety of cell types *in vitro* and *in vivo*, with very low toxicity, but this is not true of many commercially available lipids. PMD1 as we predicted was also very efficient at *in vivo* transfection, with no observed toxicity, much like MLRI. We would predict that PMD1 will also efficiently transfect a wide variety of cells, just as MLRI does. Asymmetric lipids are not necessarily best for all *in vitro* and *in vivo* gene delivery applications, but rather, given an active transfection lipid, its asymmetric counterpart is likely to be even more active. Our *in vivo* imaging results suggest that this is a viable, overlooked strategy that typically gives a boost in transfection efficiency, and a careful review of the available literature appears to support this strategy and conclusion.

Conclusions

We tested directly examples of symmetric versus asymmetric lipids *in vivo*, in this the first study that we are aware of to use live animal imaging to determine lipid transfection efficacy in brain. We present these initial results and acknowledge that further studies including additional paired symmetric and asymmetric lipids are needed. The results of this study and mini literature review, while preliminary and limited in number of lipids, fully support our suppositions and provide the basis and rationale for a larger study with additional paired symmetric versus asymmetric lipids.

Definitions

DORI, *N*-{1-(2,3-dioleoyloxy)propyl-*N*-{1-(2-hydroxy)-ethyl}-*N*,*N*-dimethyl ammonium iodide; MLRI, dissymmetric myristoyl (14:0) and lauroyl (12:0) substituted compound from the tetraalkylammonium glycerol-based cationic lipid DORI; DMRI, dimyristooxypropyl dimethyl hydroxyethyl ammonium bromide; DOTMA, *N*-{1-(2,3-dioleyloxy)propyl}-*N*,*N*,*N*-trimethlylammonium chloride; DOTAP, dioleoyloxy-3-(trimethylammonio)propane; DOPE, dioleoylphosphatidylethanolamine; DMDHP (TransFast), {bis(2-hydroxyethyl)}-*N*-methyl-*N*-{2,3-di(tetradecanoyloxy)propyl} ammonium iodide; Lipofectamine, commercial name for DOSPA, a polycationic synthetic lipid, mixed with phosphatidyl-ethanolamine, or DOPE, a fusogenic lipid with an amine-group.

Acknowledgment. Funding from NIH K08 (J.G.H.), AHA Western States (J.G.H.) and NIH R01 (J.G.H.) is gratefully acknowledged.

MP900298F

(47) Hirko, A.; Tang, F.; Hughes, J. A. Cationic lipids for plasmid gene delivery. *Curr. Med. Chem.* **2003**, *10* (14), 1185–1193.

(48) Ali, S.; Smaby, J. M.; Momsen, M. M.; Brockman, H. L.; Brown, R. E. Acyl Chain-Length Asymmetry Alters the Interfacial Elastic Interactions of Phosphatidylcholines. *Biophys. J.* **1998**, *74*, 338–348.

(49) Mui, B.; Ahkong, Q. F.; Hope, M. J. Membrane perturbation and the mechanism of lipid-mediated transfer of DNA into cells. *Biochim. Biophys. Acta* **2000**, *1467*, 281–292.

(50) Wasunga, L.; Hoekstra, D. Cationic lipids, lipoplexes and intracellular delivery of genes. *J. Controlled Release* **2006**, *116* (2), 255–264.

(51) Singh, R. S.; Mukherjee, K.; Banerjee, R.; Chaudhuri, A.; Hait, S. K.; Moulik, S. P.; Ramadas, Y.; Vijayalakshmi, A.; Rao, N. M. Anchor Dependency for Non-Glycerol Based Cationic Lipofectins: Mixed Bag of Regular and Anomalous Transfection Profiles. *Chem. Eur. J.* **2002**, *8*, 900–909.